LASER CLADDING OF THE TITANIUM ALLOY TI6242 TO RESTORE DAMAGED BLADES

Karl-Hermann Richter[1], Sven Orban[2], Steffen Nowotny[2]

[1]MTU Aero Engines, D-80995 Munich, Germany,
[2]Fraunhofer Institute for Material and Beam Technology, D-01277Dresden, Germany

Abstract

Integrally bladed rotor disks are used to an increasing extent in low-pressure compressors (LPC) and high-pressure compressors (HPC) of aero engines. These bladed disks are referred to as blisks.

One of the objectives pursued under the EU sponsored AWFORS project is to test laser cladding for its suitability to restore damaged blades of titanium blisks. This paper describes details of the laser cladding process to manufacture conventional and blade-like specimens in the titanium alloy Ti6242 and the characterization of build-up welds by evaluation of their microstructure, hardness survey and residual stress measurements.

The crucial point with regard to the application of laser cladding to replace damaged titanium blisks blades is the verification that the strength properties are not reduced. For this reason, another focus of this paper is on mechanical testing of laser clad specimens of Ti6242. Tensile and fatigue tests on conventional and blade-like specimens were performed. Both the tensile strength and the fatigue strength of laser clad specimens exceed the corresponding strength values of Ti6242 base material.

Altogether the results show that laser cladding is a highly promising technology to restore damaged blades of titanium blisks.

1   Introduction

In advanced aero engines use is made in the compressor of integrally bladed rotor disks where rotor disk and blades are one single piece. Such parts are generally referred to as blisks which is an acronym consisting of the words blade and disk. Figure 1.1 shows as an example a rotor drum comprising of two high pressure compressor blisks.

There are basically three reasons for the increasing integration of blisks in high-pressure compressors and low-pressure compressors of aero engines. The main reason is that disk rim loads are reduced and the disk can be designed accordingly, which means that the amount of weight saving is in the order up to 50%. Furthermore, in contrast to conventionally bladed rotors fretting between the disk and the blades is eliminated. Another advantage of blisks in comparison to the conventional rotor design is that there is no leakage between blades and disk which would result in a reduction of efficiency.

Figure 1.1: Rotor drum consisting of two titanium blisks.

It is an important fact that the manufacturing costs of blisks do not differ from those of conventionally bladed rotors. Depending on the size as well as on the material there are three technologies to manufacture blisks. In terms of manufacturing costs linear friction welding (LFW) is the most advantageous for the manufacture of LPC blisks in titanium. Electrochemical machining (ECM) is the most suitable manufacturing method to produce HPC blisks in nickel. High-speed cutting (HSC) is predominantly used to manufacture HPC blisks in titanium.

To repair damaged blades of a blisk, in principle the same techniques as for single blades can be used which include blending and the various conventional repair techniques to restore tip, leading and trailing edge. For

cost-effectiveness it is absolutely necessary to provide repair techniques which are capable of restoring more severe damage of a blade. In particular, such repair techniques have to be suitable for the replacement of complete blades. To date, the only existing method to replace a complete blade is LFW (1). Because of the restricted access LFW cannot be used for HPC blisks but only for LPC blisks where adequate space is available for the LFW tooling. Another potential repair technique to restore damaged blades of HPC as well as of LPC blisks is high-frequency induction pressure welding (HFIPW) which is just under development at MTU Aero Engines (2).

Laser cladding[1] is an economical and highly flexible repair technique which is already applied in the aero engine industry, e.g. to build-up worn tips of blades and labyrinth seals. For that reason, it is obvious to extend this repair technique to restore damaged blades of blisks.

The following paper presents first results of the development of laser cladding of the titanium alloy Ti6242 with a view to restoring damaged blades of blisks. The paper covers the development of the process technology and the characterization of the build-up weld as well as the results of mechanical testing which is the emphasis of this paper. All results were achieved under the EU-sponsored project Advanced Welding Technologies for Repair and Salvage (AWFORS).

2 Material
2.1 Base material

Ti6242 is a near-α titanium alloy and has an increased high-temperature strength as compared to the standard titanium alloy TiAl6V4. For this reason, Ti6242 is suitable for high-pressure compressor parts. It can be utilized up to about 450 °C (3). Table 2.1 shows the chemical composition of Ti6242.

Table 2.1: Chemical composition of the titanium alloys Ti6242. The mass rates of the chemical elements are given in %.

Element	Al	Mo	Sn	Zr	Si	Nb	O_2	C	Ti
Mass rate	5.5-6.5	1.8-2.2	1.8-2.2	3.6-4.4	0.06-0.1	----	----	----	remainder

2.2 Filler material

The Ti6242 powder was produced by electrode induction–melting gas atomization (EIGA). The characteristic of the EIGA process is the combination of gas atomization with a crucible-free melting process (4). The raw materials were rods with a diameter of 30 mm and a length of 500 mm. The powder was characterized by determination of particle size distribution, chemical analysis and evaluation of transverse sections as well as SEM examination.
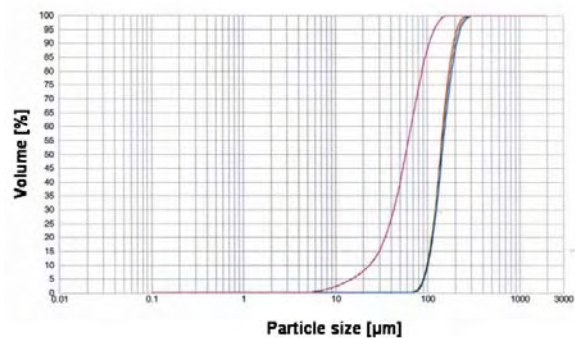

Figure 2.1: Particle size distribution of two Ti6242 powders. For all laser cladding trials the powder size fraction smaller than 100 µm (see left curve) was used.

Figure 2.1 shows the particle size distributions of Ti6242 powder. For all laser cladding trials the powder size fraction smaller than about 100 µm (see left curve in figure 2.1) was used. A spectroscopic examination showed that the mass rates of the elements within the Ti6242 powder are comparable to those of the base material. The oxygen mass ratio of the Ti6242 powder was measured by hot gas extraction. According to the results there is no oxygen contamination of the Ti6242 titanium powder. Figure 2.2 shows SEM photos of Ti6242 powder grains for two particle size fractions according to figure 2.1. The figure illustrates the round shape of the titanium powder particles.

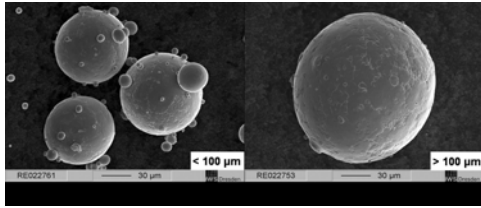[1] Laser Cladding is also known as Direct Metal Deposition (DMD).

Figure 2.2: SEM photo of Ti6242 powder grains for the two particle size distributions according to figure 2. The two particle size fractions are designated <100µm and >100µm.

3   Laser Cladding process details

For the laser cladding process a 3 KW Nd:YAG laser and the IWS coaxial cladding head type COAX8 were used. The machining system was a 4 axes precision gantry type machine equipped with the SIEMENS 840 D CNC control unit.
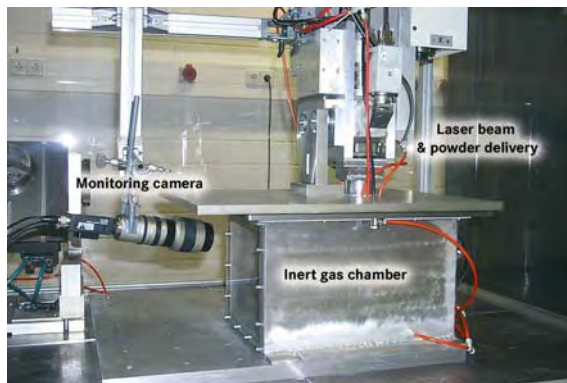

Figure 3.1: Experimental set-up for laser cladding in a sealed inert gas chamber

To protect the titanium melt from oxygen and nitrogen from the atmosphere, the process was performed in a sealed Argon gas chamber. Fig. 3.1 shows the technical set-up in the laboratory state for laser cladding of test pieces and specimens. For the repair of actual components an industrial system for controlled atmosphere laser cladding is available. In either case the residual oxygen content is less than 10 ppm.

4   Results
4.1   Manufacturing of specimens

For all mechanical tests original disk material according to an internal MTU specification was used. In the first stage, qualification disks were sectioned such that the axis of the specimens was parallel to the radial direction of the disk. Thus, it was made sure that all specimens represented actual blisk blade conditions.

4.1.1 Rectangular tensile / HCF specimens

Both tensile and HCF specimens one half of which consists of base material and built-up material (see figure 4.1) were produced as follows. Plates with the dimensions $H*W*L=40*1.5*45$ mm^3 were manufactured such that the height H of the plate corresponded to the radial direction of the qualification disk. The area W*L of the plates was laser clad.
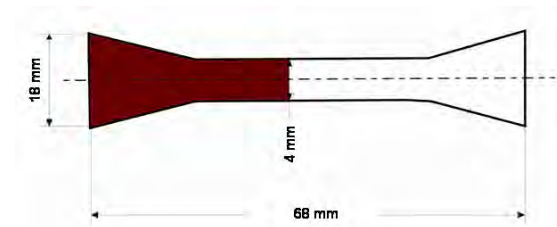

Figure 4.1: Tensile / HCF specimens used. Half of the specimens consist of laser build-up welded Ti6242 (highlighted in red).

Because the width of the surface to be laser clad was 1.5 mm single passes are sufficient to produce the laser build-up weld. In order to fixture the rectangular test pieces and to minimize the heat input the test pieces were clamped in copper shoes. In addition, the clamping device facilitates an extension of the build-up weld and therefore improves its geometry.

The deposit thickness per single pass was about 0.25-0.30 mm and did not vary from pass to pass. For that reason it was not necessary to control the height of the build-up weld during the laser cladding process. The parameters according to table 4.1 yielded the best results.

In order to avoid a superelevation of the build-up weld the laser beam was switched off at the reversal points. Because of the inertance of the powder conveyor the powder flux was not switched off at these points.

Laser type	Laser mode	Laser power	Feed rate	Powder feed rate
Nd-YAG	Continuous wave	1000 W	400 mm/min	1 g/min

After laser cladding, the specimens were thermally stress relieved according to an internal MTU specification. Then the laser clad surface was ground to fit the base plate. Finally, the tensile test specimens and the HCF test specimens were cut out (see figure 4.2).
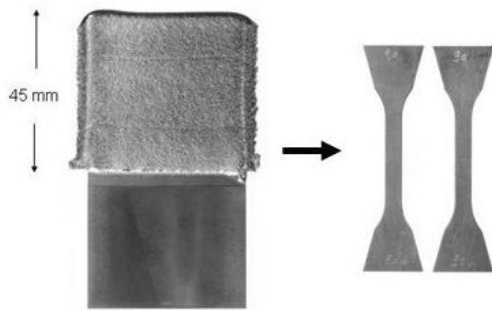

Figure 4.2: Representation of the manufacture of tensile and HCF specimens. The photo on the left shows the laser built-up plate after thermal stress relieving, that on the right shows two tensile / HCF specimens cut from the ground plate.

4.1.2   Blade-like specimens

Non-twisted blade-like test pieces are designated as 2D specimens. These specimens were defined to transfer the laser cladding process from rectangular test pieces to realistic blade geometries. To manufacture 2D specimens qualification disks were sectioned such that the axis of the blade was parallel to the radial direction of the disk. For the purpose, cuboids with the dimensions H*W*L=33*12*46 mm^3 were manufactured. The blade-like specimens produced from the cuboids by 5-axis milling were subsequently built-up by laser cladding and then post-processed to meet the final shape. Furthermore, cuboids with the dimensions H'*W*L=45*12*46 mm^3 were manufactured from which 2D reference specimens were produced which have the same shape as the laser clad 2D specimens.

To fix the 2D specimens in place and to dissipate the process heat an aligned copper clamping device was developed (see figure 4.3). It consists of two movable jaws holding the blade and a groove in which the cuboid root of the 2D specimen is fixed. Cooling water flows through the holes in the jaws and dissipates the heat caused by the laser cladding process.
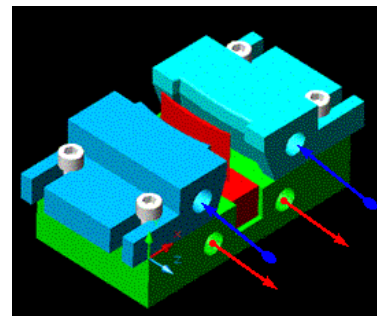

Figure 4.3: Sketch of the clamping device used for laser cladding of the 2D specimens. The blue and red arrows indicate the inflow and the drain of the cooling water, respectively.

To build-up the layer vertically the cladding process was performed in the manner described. Just as for tensile / HCF specimens the laser beam was switched off at the reversal points. The feed was additionally interrupted at these points in order to improve the heat dissipation. The holding time was about 10 seconds. Due to this interruption the growth rate of the deposition was reduced to about 1 mm/min. Because the maximum width of the profile of the blade-like specimens is comparable to the width of the HCF / tensile specimens the same laser cladding parameters could be applied (compare table 4.1).

The laser clad 2D specimens were thermally stress relieved using the same heat treatment process as for the tensile / HCF specimens. Subsequently the shape of the laser clad 2D specimens was produced by milling. Because the surface on the convex side of the laser clad and subsequently milled blade did not perfectly match the non-clad surface of the blade, the laser clad 2D specimens were manually post-processed. Figure 4.4 c shows a finish-machined laser clad 2D specimen.
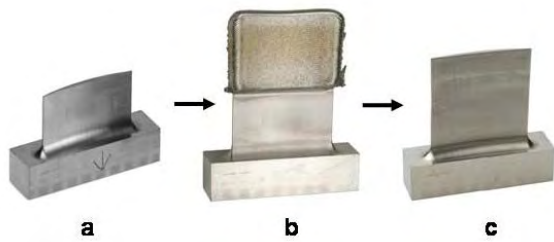
Figure 4.4: Representation of the manufacture of a*f-specimens. The photo on the left (a) shows a milled 2D specimen before laser cladding. The photo in the middle (b) shows a laser clad 2D specimen after thermal stress relieving. The photo on the right (c) shows a laser clad specimen after milling and manual post-processing.

4.2   Characterization of build-up welds
4.2.1   Welding defects

All laser clad specimens were metallic bright and showed no indications of oxidation.

A potential problem of laser cladding of titanium may be increased porosity. For this reason the porosity of the laser clad 2D specimens was assessed by transverse sections and X-ray inspection.
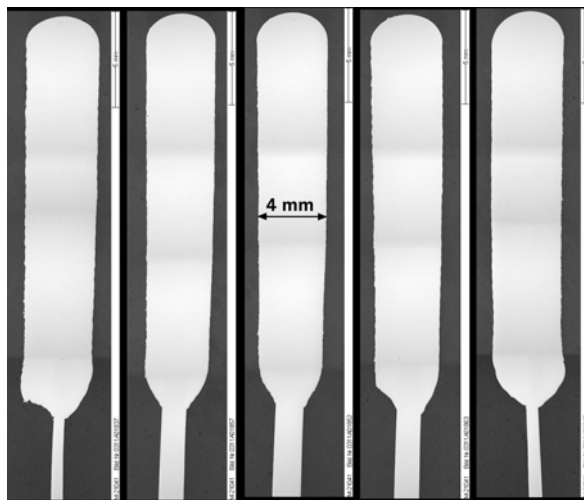

Figure 4.5: Transverse sections of a laser build-up welded 2D specimen taken from equally spaced locations . The width of the built-up layer is about 4 mm. The height is approximately 21 mm.

Figure 4.5 shows 5 transverse sections of a laser clad 2D specimen taken from equally spaced locations. The sections reveal that the laser build-up weld is slightly inclined but the final contour of the blade is definitely within the built-up weld. It is important that the transition between the base material and the build-up weld is free from notches.

Up to six pores were found per transverse section. The diameter of the pores was typically less than about 10 µm. One single pore with a diameter of about 20 µm was detected. X-ray inspection revealed no indications. Because of the small size of the pores they cannot be detected by conventional X-ray techniques.

4.2.2   Microstructure

Figure 4.6 shows a cutout of an etched transverse section in the middle of the blade close to the first pass. The bent bright fusion lines correspond to single passes lying one upon the other. The height of a single pass is in the order of 0.25-0.30 mm. Furthermore, horizontal lines are visible which are equally spaced. The distance between these lines is as large as the distance between the bright fusion lines. These horizontal lines seem to mirror the thermal heat treatment which is induced by each fusion line.
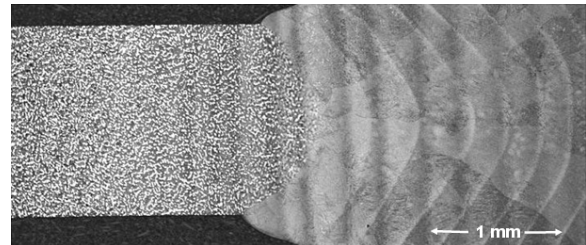

Figure 4.6: Microstructure of a laser build-up weld of a 2D specimen of the titanium alloy Ti6242.

Figure 4.6 reveals also larger grains whose grain boundaries are perpendicular to the bright fusion lines. These large grains are a consequence of the epitaxial build-up welding process.

A magnification of the build-up weld (see figure 4.7) reveals an acicular phase which is formed due to the rapid cooling conditions during the laser cladding process. This martenstic structure is known as Widmannstätten structure.

Figure 4.7: Microstructure of the melting zone of a laser build-up weld of the titanium alloy Ti624.

4.2.3 Hardness

Figure 4.8 shows a hardness survey from the base material to the build-up weld across the middle of the transverse section corresponding to figure 4.6. It reveals an approximately 20% increase in hardness from about 340 HV0.5 in the base material to about 400 HV0.5 in the built-up layer. The increase in hardness in the build-up weld is not a consequence of oxidation but due to the fine microstructure of Ti6242. Such an increase in hardness in the fusion zone is also known from other welding processes, e.g. HFIPW (2). According to figure 4.8, the width of the heat affected zone is about 2 mm.
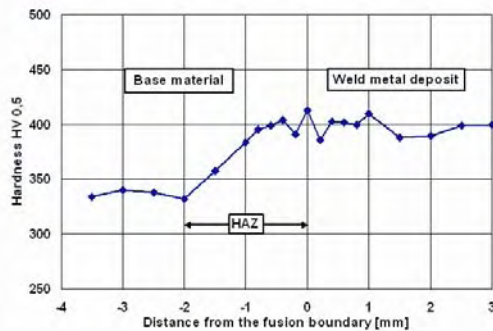

Figure 4.8: Hardness survey of laser clad 2D specimen.

4.2.4 Residual stresses

Residual stress measurements were performed using the hole drilling method. This technique allows for detecting the residual stress as a function of the depth very quickly.

Residual stresses were measured at the edges of the blades of 2D specimens in the following conditions:

- As welded (see figure 4.9 a)
- As welded + stress-relief annealed (see figure 4.9 b)
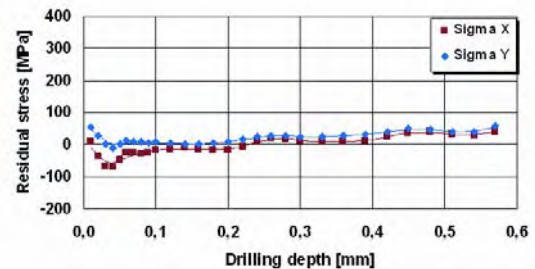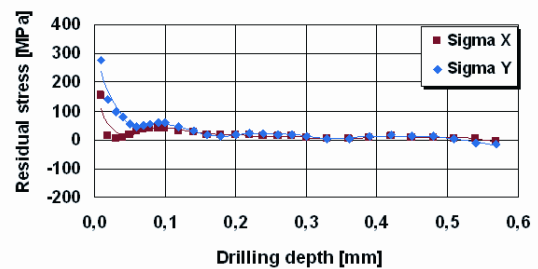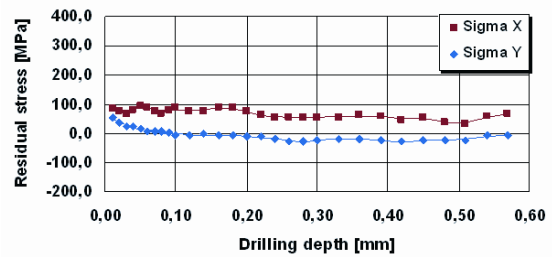- Reference specimen, not welded (see figure 4.9 c)

Figure 4.9: Residual stresses σ_x and σ_y in the conditions (a) as welded, (b) as welded and stress relief annealed and (c) not welded; σ_x is the residual stress parallel to the edge of the blade and σ_y is the residual stress perpendicular to σ_x and to the drilling direction.

The diagrams in figure 4.9 a-c show the residual stresses σ_x and σ_y in each case as a function of the drilling depth, where σ_x is the residual stress parallel to the edge of the blade and σ_y is the residual stress perpendicular to σ_x and to the drilling direction. A negative value of $\sigma_{x,y}$ means a tensile stress whereas a positive value of $\sigma_{x,y}$ means a compressive stress. The

stresses σ_x and σ_y near the surface are falsified due to mechanical machining of the surface or due to slight grinding in order to attach the strain gages. For this reason the residual stresses from 0 mm to about 0.05 mm drilling depth need not be discussed.

Figure 4.9 a shows that in the as-welded condition σ_x is about 50 - 100 MPa and σ_y is slightly negative. After stress relief annealing the residual stresses σ_x and σ_y are near to 0 MPa (see figure 4.9 b) which corresponds to the stress level of the unwelded base material (see figure 4.9 c). Due to the low stress level in the as-welded condition it may be that stress relief annealing is not stringently necessary.

4.3   Mechanical testing
4.3.1   Tensile tests

Test procedure
Tensile tests on laser clad specimens as well as on reference specimens were performed at a temperature of T=500°C using a standard testing machine.

Results
Figure 4.10 shows the results for tensile strength R_m and yield strength $R_{P0.2}$. Figure 4.11 shows the results for the elongation A. Both diagrams also include the corresponding values determined for reference specimens and the minimum values as per the MTU acceptance standard MTS1279 for the Ti6242 base material.
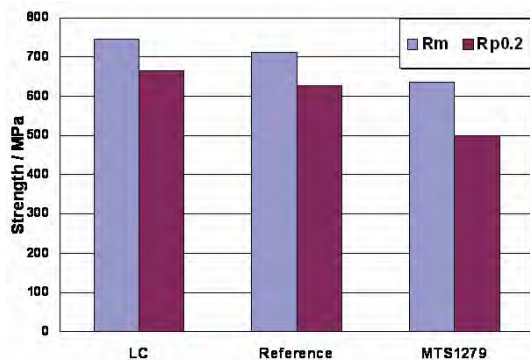

Figure 4.10: Tensile strength R_m and yield strength $R_{P0.2}$ of laser clad (LC) and reference specimens at T=500°C. In addition, the minimum tensile strength as per MTU specification is shown

As can be seen from figure 4.10, both the R_m and $R_{P0.2}$ values for laser clad specimens are higher than the corresponding values for the reference specimens. In either case the tensile strength of the laser clad specimens exceeds the minimum value as per MTU

specification. The average elongation A measured is 11.7% which is slightly less than the minimum value of 12% specified in the MTU acceptance standard. As compared with the base material the elongation of laser clad Ti6242 is reduced by about 25%.
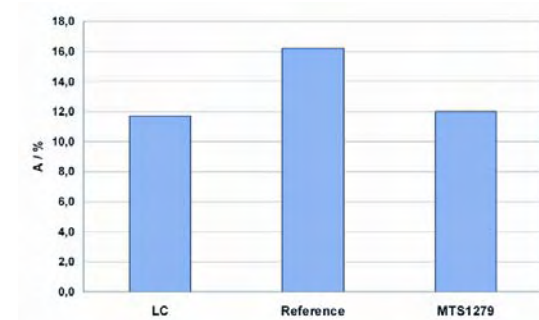

Figure 4.11: Elongation A of laser clad (LC) and reference specimens at T=500°C. In addition, the minimum elongation as per MTU specification is shown.

4.3.2   HCF tests on standard specimens

Test procedure
All HCF tests were load-controlled using a standard pulser. The stress ratio was R = 0, i.e. the stress amplitude varied between 0 and the preset maximum stress value. The test temperature was T=450°C as HCF data on the base material were already available for this temperature. HCF tests on reference specimens were not performed.

Results
The results of the HCF tests are represented in figure 4.12. All specimens fractured outside the build-up weld in the base material. Thus, the fatigue strength of the laser clad specimens apparently exceeds that of the base material. As can be seen from the diagram the fatigue strength of the Ti6242 material used here is slightly higher than that of the previously tested Ti6242 material.

4.3.3   HCF tests on blade-like specimens

Test procedure
The objective of HCF tests on blade-like specimens is to determine the minimum fatigue limit of blades. In the aero engine industry these tests are designated as a*f tests. For statistical reasons at least 5 a*f tests should be performed on actual parts and on reference parts to determine the fatigue strength $\mu - 2*\sigma$ where μ is the average value and σ the standard deviation.
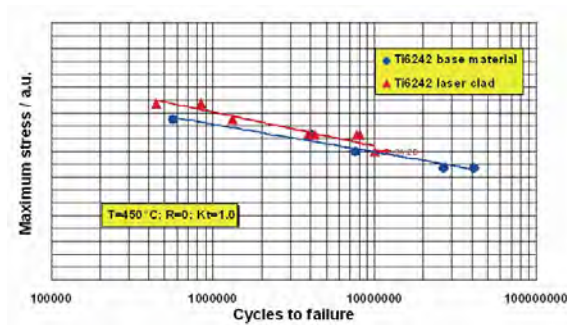
Figure 4.12: HCF data of laser clad Ti6242 as compared with already tested Ti6242 base material. The fact that the specimens fractured outside the build-up weld indicates that the Ti6242 material used has a slightly better fatigue strength than the previously tested Ti6242 base material. The maximum stress is shown in arbitrary units (a.u.). The data points with arrows correspond to specimens that have passed 10 million cycles.
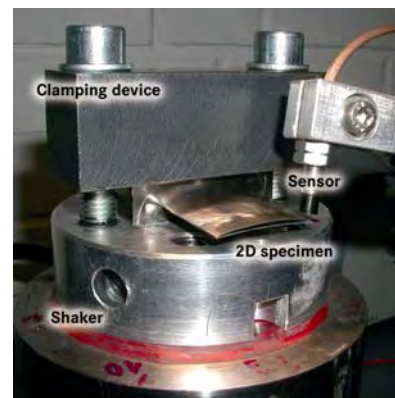

Figure 4.13: Shaker test rig used for a*f-tests. The photo shows a clamped 2D specimen and an eddy-current sensor for measurement of the oscillation frequency of the blade

The advantage of a*f tests is that the specimens tested are actual blades. The test procedure is similar to that of a fatigue test. The specimen is excited to a preset eigenfrequency with a preset amplitude. After a pre-determined number of cycles the amplitude is increased and the specimen is again subjected to the same number of cycles. The procedure is repeated until the eigenfrequency drops off. The frequency is measured by an eddy-current sensor. In general, the frequency drop-off corresponds to a crack initiated by fatigue. The specimen is then subjected to fluorescent penetration indication to conform incipient cracking.

All a*f tests on 2D specimens were carried out at room temperature both on laser clad specimens and on reference specimens. The specimens were fixed at the cuboid and excited by a shaker test rig to the preset eigenfrequency. Figure 4.13 shows the experimental set-up.

Results
To verify the behaviour of the laser clad blade tip it was decided to perform a*f tests in the so-called 1C mode. This eigenfrequency corresponds to a flexural mode showing two nodal points at the tip of blade and is approximately 11.0 kHz. Figure 4.14 shows the result of a finite-element method calculation applied to the 2D specimens oscillating in the 1C mode. The diagram on the left shows the displacement which is at a maximum at the leading and trailing edges. The photo on the right shows the stress distribution with a maximum in the middle of the blade tip.
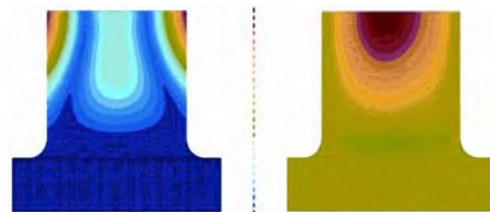

Figure 4.14: Calculated displacement distribution (left-hand diagram) and stress distribution (right-hand diagram) of the 2D specimen stimulated in the 1C mode. The results of the FEM calculation indicate that cracks start from the middle of the tip. Green (red) color means low (high) stress. Blue (red) color means low (high) displacement.

Figure 4.15 shows the displacement of a 2D specimen stimulated to the 1C mode measured by holographic interferometry. As can be seen there is a perfect match between the calculated and the measured displacement distribution. In either case the crack initiation is expected to occur in the middle of the blade tip.

In contrast to tensile and HCF tests, a*f tests cause incipient cracking in the laser build-up weld, in either case. As expected all incipient cracks started from the middle of the blade tip, irrespective of whether a reference specimen or a laser clad specimen was tested.
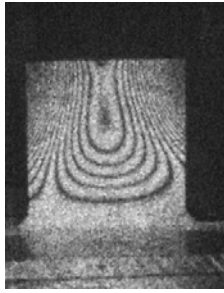
Figure 4.15: Holographic-interferometric measurement of the displacement distribution of the 2D specimen stimulated in the 1C mode. The experimental result corresponds perfectly to the results of the FEM calculation (compare left-hand diagram of figure 4.14).
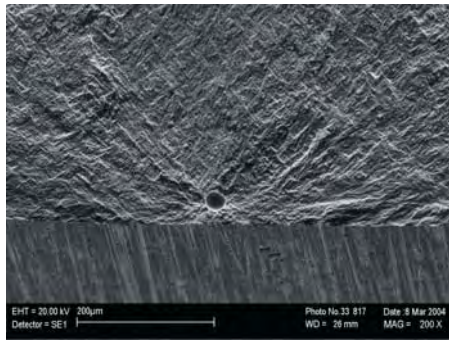

Figure 4.16: SEM micrograph of an incipient crack in a laser clad 2D specimen. The crack starts from a pore just below the surface. The diameter of the pore is in the order of 20 μm.

The cracks in all a*f-tested laser clad 2D specimens started from pores. Figure 4.16 shows, as an example, an SEM micrograph of an incipient crack in a laser clad 2D specimen.

Figure 4.17 summarizes the results of a*f tests. The minimum fatigue strength, $\mu - 2*\sigma$, of the laser clad specimens is about 14% higher than that of the Ti6242 base material! For reference, figure 4.17 also shows the minimum fatigue strength of an actual high-pressure compressor blade from which the 2D speci-mens were derived. As can be seen from the diagram the minimum fatigue strength of the actual blade is practically equal to the minimum fatigue strength of the laser clad 2D specimen. In contrast to the actual blade both the laser clad specimens and the reference specimens were not post-processed by shot peening which induces compressive stress and therefore im-proves minimum fatigue strength.
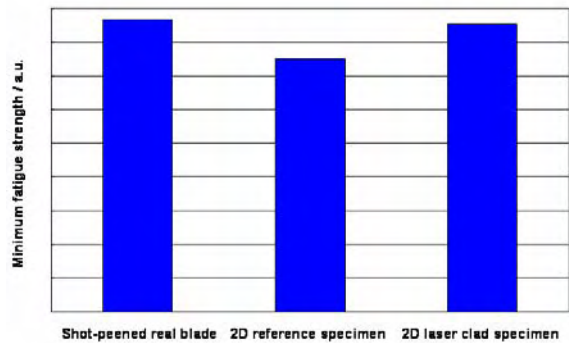

Figure 4.17: Minimum fatigue strength of 2D Ti6242 reference specimens, laser clad 2D specimens and actual high-pressure compressor blades from which the 2D specimens were derived. In contrast to the actual blades the 2D specimens were not post-processed by shot peening.

5 Conclusion and outlook

The study shows that laser cladding of the high temperature titanium alloy Ti6242 produces excellent build-up welds with very low porosity. Due to the results of the strength tests laser build-up welds exceed both the tensile and the fatigue strength of the Ti6242 base material. For this reason, laser cladding has the potential to restore damaged blades of blisks.

The results of this study cover only the titanium alloy Ti6242. Because of the similar welding behaviour of all conventional titanium alloys which are used in compressors of aero engines it is obvious to suppose that the existing results can be transferred to all near-α and (α+ß) titanium alloys, e.g. TiAl6V4, Ti6246, IMI834, etc.

To date the height of the laser build-up weld was about 40% of the total height of the blade. In order to test the potential of this repair process to replace full blisk blades, 80% of the total height of an original HPC blisk blade will be built-up by laser cladding in the next step of the AWFORS project. It is planned to perform a*f tests on these blades in another flexural mode.

References

(1) D. Schneefeld, D. Helm and H. Wilhelm, Linear Friction Welding of Compressor Stages in Titanium Alloys

(2) U.C. Knott, Inductive High Frequency Pressure (IHFP) Welding for Blisk Maintenance, DVS-Berichte Vol. 229 (2004), pp. 72-76

(3) M. Peters, Modern Titanium Alloys for High Temperatures, Metall Vol. 42, No. 6 (1988), pp. 576-581.

(4) See http://www.tls-technik.de